Aalborg Universitet

AALBORG UNIVERSITY

Absorption Cycle Heat Pump Model for Control Design

Vinther, Kasper; Just Nielsen, Rene; Nielsen, Kirsten Mølgaard; Andersen, Palle; Pedersen, Tom Søndergård; Bendtsen, Jan Dimon

Absorption Cycle Heat Pump Model for Control Design

Kasper Vinther[1], René J. Nielsen[2], Kirsten M. Nielsen[1], Palle Andersen[1],
Tom S. Pedersen[1] and Jan D. Bendtsen[1]

Abstract— Heat pumps have recently received increasing interest due to green energy initiatives and increasing energy prices. In this paper, a nonlinear dynamic model of a single-effect LiBr-water absorption cycle heat pump is derived for simulation and control design purposes. The model is based on an actual heat pump located at a larger district heating plant. The model is implemented in Modelica and is based on energy and mass balances, together with thermodynamic property functions for LiBr and water and staggered grid representations for heat exchangers. Model parameters have been fitted to operational data and different scenarios are simulated to investigate the operational stability of the heat pump. Finally, this paper provides suggestions and examples of derivation of lower order linear models for control design.

I. Introduction

Energy consumption in residential, commercial and industrial buildings has received increasing attention in recent years due to the rising demand for efficient energy use and higher comfort standards. In industrial buildings, in particular, energy efficiency is becoming more and more important in order to avoid waste. Due to their attractive properties, heat pumps of various types are seeing extensive use in modern buildings, see for instance [1], [2], and many others. Furthermore, applying heat pumps together with other technologies at modern combined heat and power (CHP) plants and using them in combination with district heating, can yield significant economical and practical benefits, as described in e.g. [3], [4], [5], [6], and [7].

The town of Sønderborg in the southern part of Denmark is one such case, where two suppliers, Sønderborg Fjernvarme (SFJV) A.m.b.a. and Sønderborg Kraftvarmeværk I/S, collaborate to provide district heating to a fairly large number of commercial and private consumers in the local area. Together, the two suppliers incorporate burning of waste, natural gas, wood-chips and, of highest relevance to the present paper, four interconnected *absorption cycle heat pumps* primarily driven by geothermal heat.

As can be expected, day-to-day operation needs to be adjusted to consumer load changes, weather, fuel prices, etc. In order to operate complex plants under such dynamic conditions, it is necessary to have good knowledge of the

[1]K. Vinther, K. Nielsen, P. Andersen, T. Pedersen and J. Bendtsen are with the Section of Automation and Control, Department of Electronic Systems, Aalborg University, 9220 Aalborg, Denmark {kv,kmn,pa,tom,dimon}@es.aau.dk
[2]R. Nielsen is with Added Values, 7100 Vejle, Denmark RJN@AddedValues.eu

dynamic behavior and constraints of individual units. However, while absorption cycle heat pumps have received some attention in terms of modeling for the purpose of design and operation under steady state conditions, the literature is quite limited when it comes to modeling for control purposes. [8] and [9] provides an overview of the technology, but does not consider dynamic operation; [10], [11], and [12] all provide steady-state models of absorption cycle heat pumps of varying degree of detail, but also do not consider dynamics. [13] and [14] both present models that include dynamics (mass storage and thermal inertia), but the main focus remains on steady-state operation.

In this paper, we present a single-effect absorption cycle heat pump model for the specific purpose of investigating control design issues. In our model, the main heat transport is carried out by a chemical absorption/desorption cycle involving a mixture of water and Lithium-bromide (LiBr), and we consider both mass storage and heat transfer. The model is implemented as interconnected components in the simulation tool *Dymola* using the open-source and object-oriented modeling language *Modelica* [15]. The component models of the absorber and generator are formulated based on the aforementioned modeling papers, while the evaporator and condenser models are inspired by [16]. Heat exchangers are modeled using staggered grid models, e.g., see [11], while LiBr properties are modeled according to [17]. Model parameters are then fitted using actual plant data.

The outline of the paper is as follows. Section II gives an overview of the heat pump process. Section III presents the main model components, whereupon Section IV presents the results of parameter fitting. Next, Section V shows simulations with external water flow control, Section VI discusses linearization of the model, and Section VII sums up the work. Finally, it should be pointed out that a companion paper, [18], presents an analysis of different control loop configurations based on the model presented here.

II. District Heating Heat Pump Setup

At the highest level of abstraction, a part of the district heating supply system at SFJV is structured as shown in Fig. 1. The main sources of heat are a wood-chip fired boiler (high-value heat) and a geothermal reservoir (low-value heat). These two main heat sources supply heat to the district heating system via four absorption cycle heat pumps interconnected in a fairly complex way that permits one or more of the individual heat pumps (of different size) to be disengaged from the heat supply operation. In the following, we will limit our focus to the largest heat pump (HP1).
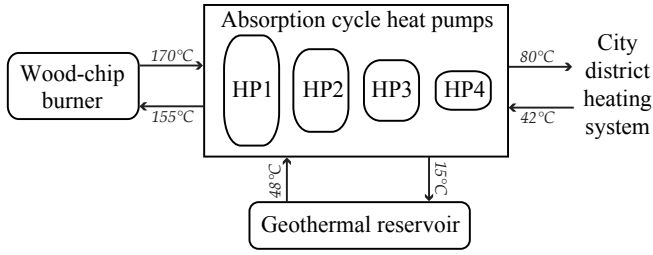
Fig. 1. Bird's eye view of a district heat supply system at SFJV with indication of typical water flow temperatures.

Fig. 3. Dühring chart illustration of different state points in the absorption cycle. The four colored dots indicate the initial conditions of the liquid content of the evaporator, absorber, generator, and condenser for the data presented in Section V.

The heat pump in question was delivered by Hope Deep-blue Air-conditioner Manufacture Corp., Ltd., and has an operational weight of 67 ton [19]. An illustration of the heat pump is provided in Fig. 2. The basic absorption cycle works similarly to the standard vapor compression cycle except that the compressor is replaced by an absorber and a generator, and the working fluid in an absorption refrigeration system is a binary solution consisting of refrigerant and absorbent—in this case, water and LiBr, respectively. This solution is pumped from the absorber to the generator by an electrical pump $(1 - 3)$. High temperature water from the wood-chip burner is supplied to the generator $(11 - 12)$ and used to evaporate refrigerant out from the solution. The refrigerant and absorbent are chemically separated as the refrigerant vaporizes, leaving a liquid solution with a high absorbent concentration in the generator, which is gradually returned to the absorber (4) when the generator overflows. A u-tube mechanism then helps maintain a pressure difference between the generator and absorber $(5 - 6)$, see [13] for

further explanation of the u-tube design. The refrigerant vapor from the generator is led to a condenser (7), where a standard condensation occurs, expelling heat to the surroundings $(15 - 16)$, which in this case is district heating water. Saturated refrigerant is fed to an evaporator through another u-tube overflow mechanism $(8 - 9)$, where it evaporates, consuming heat from the surroundings $(17 - 18)$. Actually, in this case, heat is taken from the district heating water, but this water is reheated by geothermal water, which can be considered as a cheap energy source. An evaporator pump is used to continuously circulate liquid refrigerant across the heat exchanger pipes. Finally, the vapor is led to the absorber (10), where the solution absorbs refrigerant vapor at low pressure; this absorption process is an exothermic process. This means that it must reject heat to the surroundings $(13 - 14)$, which again is district heating water. A solution heat exchanger (HEX) allows the solution from the absorber (2) to be preheated before entering the generator (3) by using the heat from the hot solution leaving the generator $(4-5)$. As a consequence, less hot water from the wood-chip burner is required in the generator. Moreover, the size of the absorber can be reduced as less heat is rejected. The system also has a water HEX located after the condenser, which transfers heat from the refrigerant to the district heating water $(19 - 20)$ before it enters the evaporator.

Fig. 3 shows a Dühring chart, which is a graphical representation of the pressure/temperature/concentration at different saturated state points in the absorption cycle. Note the red curve; it indicates at which combinations of concentration, pressure, and temperature the LiBr solution starts to crystallize, which can result in clogging of the pipes and interruption of machine operation. The region of operation below this curve should thus be avoided and the critical point is where the strong solution returns to the absorber.

III. ABSORPTION CYCLE HEAT PUMP MODEL

A sketch of a single-effect LiBr-water absorption cycle heat pump model is shown in Fig. 4. The individual components are drawn in a temperature-pressure diagram to illustrate the relative operating conditions in the four main components (evaporator, absorber, generator, and condenser).
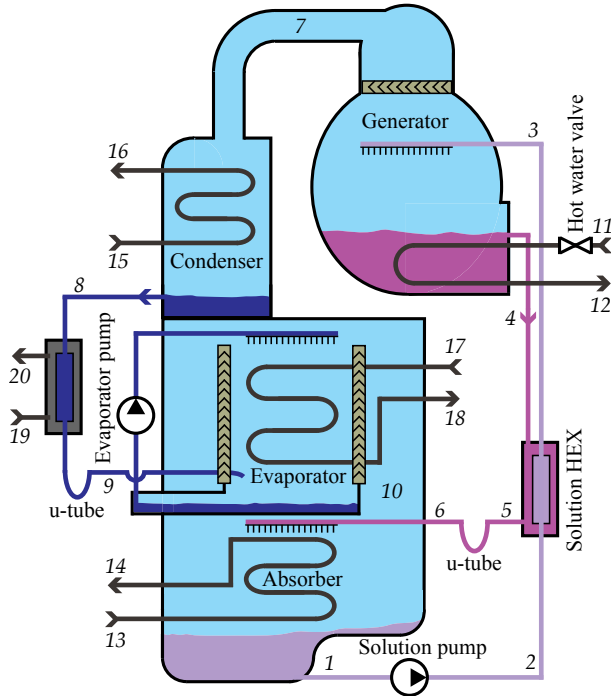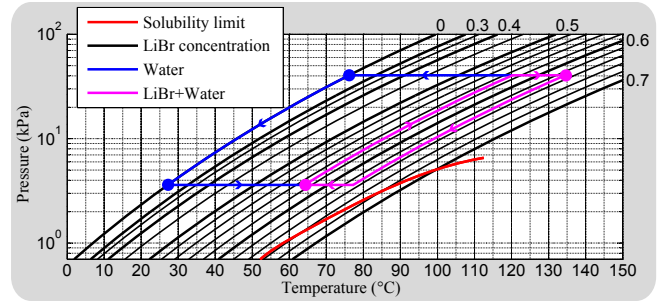

Fig. 2. Illustration of the absorption cycle heat pump at SFJV. The numbers indicate thermodynamic state points used in the model (adopted from [8]).
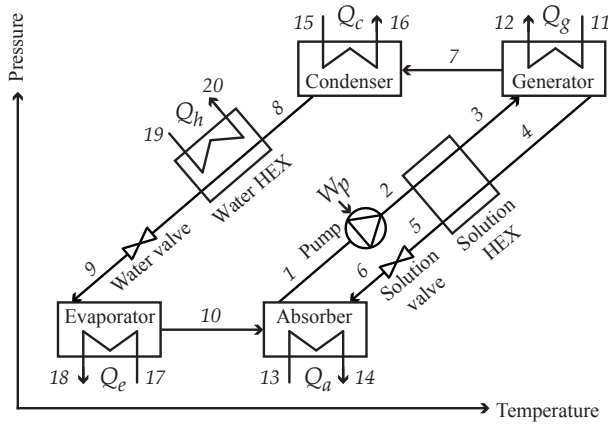
Fig. 4. A sketch of the absorption heat pump model drawn in a temperature-pressure diagram. The numbers indicate state points used in the model.

The model is based on the heat pump system shown in Fig. 2. However, for simplicity, the evaporator with evaporator pump is replaced by an evaporator model without the pump, where the heat exchanger pipes are submerged in the liquid water. The overflow pipes from the generator and the condenser together with the u-tube design can alternatively be replaced by controlled electronic expansion valves. Valve models are therefore used, where control loops start to open the valves, when the level in the generator or the condenser exceeds a predefined upper bound (nominal level).

The dynamic model of the absorption cycle used in this work is based on mass and energy balances and thermodynamic property functions. Further, the model is implemented in the *Modelica* modeling language. This allows reuse of the standard `Fluid` and `Media` libraries and encourages object-oriented programming. Fluid flow between individual component models in thermodynamic systems are also standardized using the stream connector implementation, see [20], which is also adopted here.

In the following it is assumed that the evaporator and absorber operate at the same low pressure, and that the generator and condenser operate at the same high pressure. Further, there are no heat losses to the ambient air and each of the four main components can be represented by a liquid control volume (subscript l) and a vapor control volume (subscript v). The overall mass balances are

$$\text{Eva:} \quad \frac{dM_e}{dt} = m_9 - m_{10}, \qquad (1)$$

$$\text{Abs:} \quad \frac{dM_a}{dt} = m_6 + m_{10} - m_1, \qquad (2)$$

$$\text{Gen:} \quad \frac{dM_g}{dt} = m_3 - m_4 - m_7, \qquad (3)$$

$$\text{Con:} \quad \frac{dM_c}{dt} = m_7 - m_8, \qquad (4)$$

$$M_i = V_{i,l}\rho_{i,l} + V_{i,v}\rho_{i,v} = V_{i,l}\rho_{i,l} + (V_{i,tot} - V_{i,l})\rho_{i,v} \quad (5)$$

where M is mass, V is volume, ρ is density, m correspond to mass flows illustrated with arrows in Fig. 4, $i \in \{e, a, g, c\}$ in (5) and (12) denote each component, and subscript tot

denotes total. The LiBr mass balances are

$$\text{Abs:} \quad \frac{d(X_a V_{a,l}\rho_{a,l})}{dt} = X_6 m_6 - X_1 m_1, \qquad (6)$$

$$\text{Gen:} \quad \frac{d(X_g V_{g,l}\rho_{g,l})}{dt} = X_3 m_3 - X_4 m_4, \qquad (7)$$

where X is mass fraction of LiBr. The energy balances are

$$\text{Eva:} \quad \frac{dU_e}{dt} = m_9 h_9 - m_{10} h_{10} + Q_e, \qquad (8)$$

$$\text{Abs:} \quad \frac{dU_a}{dt} = m_6 h_6 + m_{10} h_{10} - m_1 h_1 - Q_a, \qquad (9)$$

$$\text{Gen:} \quad \frac{dU_g}{dt} = m_3 h_3 - m_4 h_4 - m_7 h_7 + Q_g, \qquad (10)$$

$$\text{Con:} \quad \frac{dU_c}{dt} = m_7 h_7 - m_8 h_8 - Q_c, \qquad (11)$$

$$U_i = V_{i,l}\rho_{i,l}h_{i,l} + V_{i,v}\rho_{i,v}h_{i,v} - p_i V_{i,tot} \qquad (12)$$

where U is internal energy, Q is heat transfer rate, h is specific enthalpy, and p is pressure.

The water vapor flow out of the generator solution and the water vapor flow absorbed in the absorber are driven by the amount of heat transferred through the HEXs assuming that the solutions are always in a saturated state. It is also assumed (see [8]) that the solution that exits the absorber and generator, the water that exits the condenser, and the vapor that exits the evaporator, all are in a saturated state (same state as in the respective components). Additionally, the vapor from the generator interacts with the solution from the absorber in a counterflow way (sprayed in), such that the vapor at the outlet is superheated to the saturation temperature of the solution, see again [8].

The mass and energy balances are supplemented with thermodynamic property functions. E.g., to calculate enthalpy or density of water we would use a function of the form

$$(h, \rho) = f(p, T),$$

since liquid-vapor equilibrium is assumed. The water property functions are part of the standard *Modelica* `Media` library and the LiBr-water solution property functions are implemented based on the formulations given in [17].

Since `Modelica.Media` does not provide an interface for incompressible solutions the LiBr-water solution properties have been implemented in a separate package with functions for pressure, $p(T, X)$, density $\rho(T, X)$, specific enthalpy $h(T, X)$, entropy $s(T, X)$ and heat capacity $c_p(T, X)$. Their partial derivatives wrt. temperature, T, and concentration, X, have been symbolically deduced from the expressions in [17] and are also provided in the package.

The HEX in the four main components, the water HEX, and the solution HEX, illustrated in Fig. 4, are such that partial differential equations must be used in the description due to the distributed parameter nature. This is modeled using 1-dimensional dynamic staggered grid flow models with a finite volume model representation with N volumes elements (volume divided equally) and $N + 1$ flow elements in between the volumes, as shown in Fig. 5. Further, stream connectors are used to connect each element as indicated
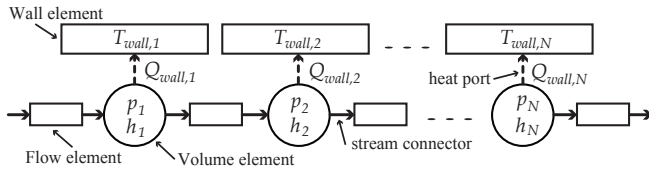
Fig. 5. Illustration of a *Modelica* implementation of a 1-dimensional staggered grid model connected to a wall.

and heat ports are used for the connection of the volume elements with the wall elements.

The energy balance equation for the j'th volume element in the staggered grid model, $j = 1, \ldots, N$, is;

$$\frac{d\left(\frac{V_{tot}}{N}\rho_j h_j - p_j \frac{V_{tot}}{N}\right)}{dt} = m_{j-1}h_{j-1} - m_j h_j + Q_{wall,j}, \tag{13}$$

$$Q_{wall,j} = \frac{UA}{N}(T_{wall,j} - T_j), \tag{14}$$

$$UA = UA_{no}\left(\frac{|m_j|}{m_{no}}\right)^{0.8}, \tag{15}$$

where UA is a mass flow dependent overall heat transfer coefficient, subscript $_{no}$ defines nominal values, and T_{wall} is pipe wall temperature. Inlet and outlet pressures are equal for each volume and the outlet temperature of each volume is equal to the temperature of that volume T_j. Furthermore, the pipe wall temperature is modeled by

$$\frac{M_{wall}}{N}c_{p,wall}\frac{dT_{wall,j}}{dt} = Q_{wall,in,j} - Q_{wall,out,j}, \tag{16}$$

where $Q_{wall,in}$ and $Q_{wall,out}$ are the heat transfer rate into and out of the wall, respectively, and $c_{p,wall}$ is the specific heat capacity of the wall material. To keep the model simple, the water heat exchangers for the four main components are assumed to have saturation temperature along the entire length of the secondary side of the wall (internal heat pump temperature). Steady state mass balance is also assumed in each staggered grid model, since only incompressible fluid flows occur in these.

The pressure drop Δp_j across the j'th flow element in the staggered grid model, $j = 1, \ldots, N+1$, located between the N volume elements, is calculated as

$$\Delta p_j = \frac{K_f}{\rho_j}m_j|m_j|, \tag{17}$$

where K_f is a fixed flow coefficient for each flow element. Note that the pressure loss internally in the heat pump cycle between state points 2-3, 4-5, and 8 to before the water valve are assumed to be negligible and thus set to zero, together with static mass balances. This reduces model complexity considerably and improves simulation speed.

A linear static equation is used to describe the mass flow rate through the valves;

$$K_v m_v = \alpha \Delta p_v, \tag{18}$$

where K_v is a fixed flow coefficient, m_v is mass flow through the valve, α is valve opening degree, and Δp_v is the differential pressure across the valve.

Finally, the mass flow through the solution pump m_1 is related to the pump work W_p via the static equation

$$\eta_p W_p = \Delta p_p \frac{m_1}{\rho_p}, \tag{19}$$

where η_p is a fixed pump efficiency and ρ_p is the density of the incompressible solution.

IV. MODEL PARAMETER FITTING AND COMPARISON WITH OPERATIONAL DATA

The heat pump model described in Section III contains multiple parameters that can represent the operational characteristics of a given system. Data from the heat pump described in Section II and a data sheet [19] are used to fit the parameters to HP1 (Fig. 1) located at SFJV. In addition to identification of parameters, it is necessary to implement and tune basic stabilizing control loops similar to the setup in SFJV, because the available data is obtained from closed-loop operation. However, once a basic control setup is found that provides a good fit to the closed-loop data it can be used as a benchmark for design of more advanced control.

The mass flow through the solution pump m_1 is used to control the LiBr concentration of the strong solution at the outlet of the generator, while the external water mass flow through the generator m_{11} is used to control the condenser pressure (same pressure as in the generator). The external water mass flow through the water HEX m_{19} is controlled to maintain a constant outlet temperature T_{20}.

Decentralized PI control loops are used for each of the mass flows (m_1, m_{11}, and m_{19}) to provide simple setups that can be tuned manually. Note that the exact control algorithms in the heat pump at SFJV are unknown and the suggested control implementation is only one out of many possible ways to control the cycle, see [18] for further detail on potential control setups. However, the suggested controls have given the best agreement between data and simulation.

Finally, the external water mass flow through the evaporator, absorber, and condenser are controlled externally as described in Section V and the data presented in Fig. 6
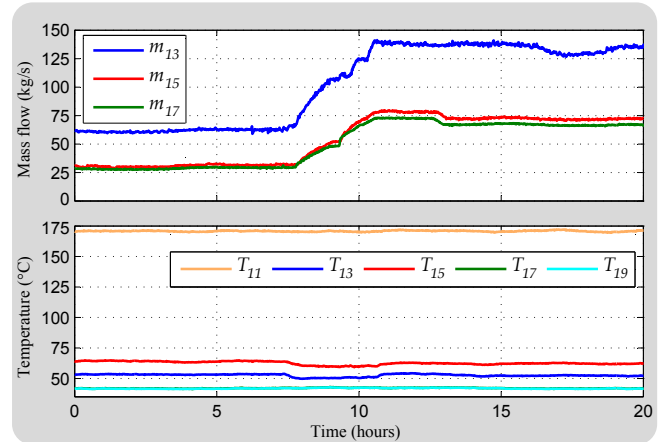

Fig. 6. Measured external water mass flow and inlet temperatures during 20 hours of operation of the heat pump at SFJV.

are used as input to the simulation, along with the initial conditions shown in Fig. 3.

Table I contains the most important model parameters. The volumes and HEX wall masses are based on information provided in the data sheet [19]. The relative sizes of the solution HEX and the water HEX are assumed to be 10% of the generator and condenser sizes, respectively. Furthermore, it is assumed that the nominal liquid filling (level) of the evaporator, absorber, and condenser is 15% of their respective total volumes. The generator has a slightly higher nominal liquid level of 20%. The resulting masses of HEX walls, water, solution, and miscellaneous equipment gives reasonable total shipment and fluid weight values, respectively 54.6 ton and 12.4 ton, when compared with data sheet values. The heat transfer parameters and the control parameters were found through manual iteration from an initial guess to give a good visual fit in steady state operation and in the transient behavior during the ramp change in capacity utilization during the 20 hours of operation (see Fig. 6). In addition, 7 volume elements and 8 flow elements are used to discretize the HEX tubes, which is a trade-off between model accuracy and complexity (the improvement in accuracy is negligible with more elements).

The simulation result using the manually tuned model parameters is compared with operational data from SFJV in Fig. 7. Only four measurements are available internally in the heat pump cycle (T_4, T_8, T_{10}, and X_4). This means that the initial absorber concentration has also been an iteration variable in the model tuning process and it was set to 55.5% in the presented simulation result. A potential set point reference for the concentration $X_{4,ref}$ used at SFJV is unknown and the control loop in the simulation has therefore been set to follow the measured concentration at SFJV as reference. However, the reference for the condenser pressure control loop is kept fixed at the initial pressure.

Changes in all temperatures are observed when the capacity is ramped up at around 7 hours. The system settles again a couple of hours after the ramping period ends at around 11 hours. All the temperatures show good qualitative agreement with measurement data. The largest offsets are seen in the temperatures associated with the generator and absorber. These models are relatively simple, where the temperature of the solution is assumed to be the same across the entire HEX wall. Models with higher fidelity could be used; however, this will increase the model order and the obtained model detail is considered adequate for control design.

V. SIMULATION OF EXTERNAL WATER FLOW CONTROL

The external evaporator water mass flow m_{17} is used to determine the desired capacity utilization of the heat pump. Higher external mass flow through the evaporator generates more steam, which in turn requires a higher absorber flow to absorb the steam and a higher condenser flow to generate enough condensate for the evaporator. Higher condensation rate in the condenser lowers the pressure and the internal control will thus generate more steam in the generator and pump more solution from the absorber to maintain a suitable

Parameter	Description	Value	Unit
Geometry			
$V_{e,tot}$	Total eva. volume	8.516	m^3
$V_{a,tot}$	Total abs. volume	9.770	m^3
$V_{g,tot}$	Total gen. volume	6.882	m^3
$V_{c,tot}$	Total con. volume	6.557	m^3
$M_{e,wall}$	Mass of eva. HEX wall	11355	kg
$M_{a,wall}$	Mass of abs. HEX wall	13026	kg
$M_{g,wall}$	Mass of gen. HEX wall	9176	kg
$M_{c,wall}$	Mass of con. HEX wall	8742	kg
$M_{w,wall}$	Mass of wat. HEX wall	917.6	kg
$M_{s,wall}$	Mass of sol. HEX wall	917.6	kg
$c_{p,wall}$	Specific heat cap. of HEX walls	510	$\frac{J}{kgK}$
Heat Transfer			
$UA_{e,no}$	Nom. eva. HEX heat transf. coef.	1.5×10^6	$\frac{W}{K}$
$UA_{a,no}$	Nom. abs. HEX heat transf. coef.	2.2×10^6	$\frac{W}{K}$
$UA_{g,no}$	Nom. gen. HEX heat transf. coef.	2×10^6	$\frac{W}{K}$
$UA_{c,no}$	Nom. con. HEX heat transf. coef.	2.5×10^6	$\frac{W}{K}$
$UA_{w,no}$	Nom. wat. HEX heat transf. coef.	1.7×10^5	$\frac{W}{K}$
$UA_{s,no}$	Nom. sol. HEX heat transf. coef.	1.5×10^5	$\frac{W}{K}$
$m_{17,no}$	Nom. ext. eva. HEX mass flow	116	$\frac{kg}{s}$
$m_{13,no}$	Nom. ext. abs. HEX mass flow	184	$\frac{kg}{s}$
$m_{11,no}$	Nom. ext. gen. HEX mass flow	151	$\frac{kg}{s}$
$m_{15,no}$	Nom. ext. con. HEX mass flow	125	$\frac{kg}{s}$
$m_{19,no}$	Nom. ext. wat. HEX mass flow	3.5	$\frac{kg}{s}$
$m_{8,no}$	Nom. int. wat. HEX mass flow	2.6	$\frac{kg}{s}$
$m_{2,no}$	Nom. weak sol. HEX mass flow	20.8	$\frac{kg}{s}$
$m_{4,no}$	Nom. strong sol. HEX mass flow	18.2	$\frac{kg}{s}$

LiBr concentration in the generator. The heat pump located at SFJV is specified to operate with external absorber and condenser mass flows as a scaling of the evaporator mass flow with minimum and maximum margins;

$$0.95 k_a m_{17} \leq m_{13} \leq 1.6 k_a m_{17}, \qquad (20)$$

$$0.85 k_c m_{17} \leq m_{15} \leq 1.15 k_c m_{17}, \qquad (21)$$

with nominal absorber flow scaling $k_a = 1.591$ and nominal condenser flow scaling $k_c = 1.078$.

In order to keep the heat pump operable it is important that the liquid levels (mass distributions) in each of the four main components are kept within a reasonable range from their nominal values. It is also important that the concentration is controllable to be able to prevent potential crystallization.

Simulations of the four extreme situations in terms of absorber and condenser mass flow are shown in Fig. 8. The simulation conditions are the same as presented in Section II, except for the external absorber and condenser mass flows, which are set to be scaled according to Eq. (20) and (21).

The levels and concentration are kept within reasonable bounds during the 20 hour simulations in three out of four extreme cases. The situation with high condenser mass flow and low absorber mass flow exhibits potential problems in
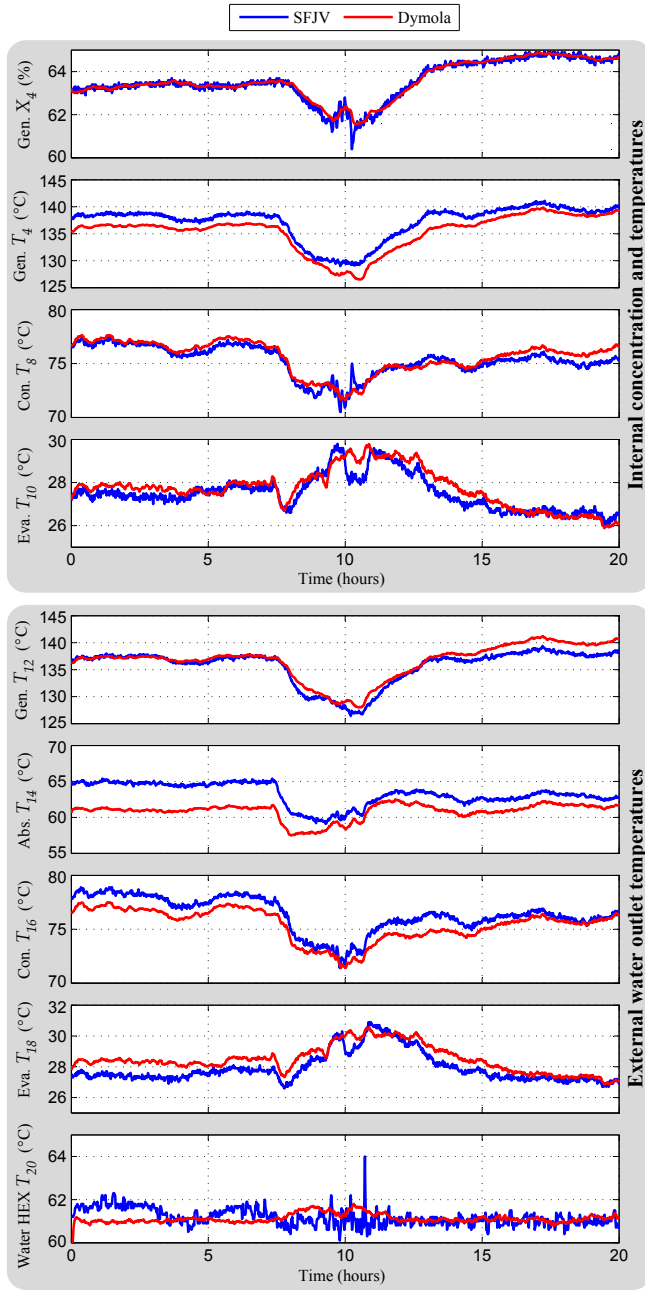
Fig. 7. Comparison between 20 hours of data from SFJV and simulation data from the absorption cycle heat pump model in *Dymola*.
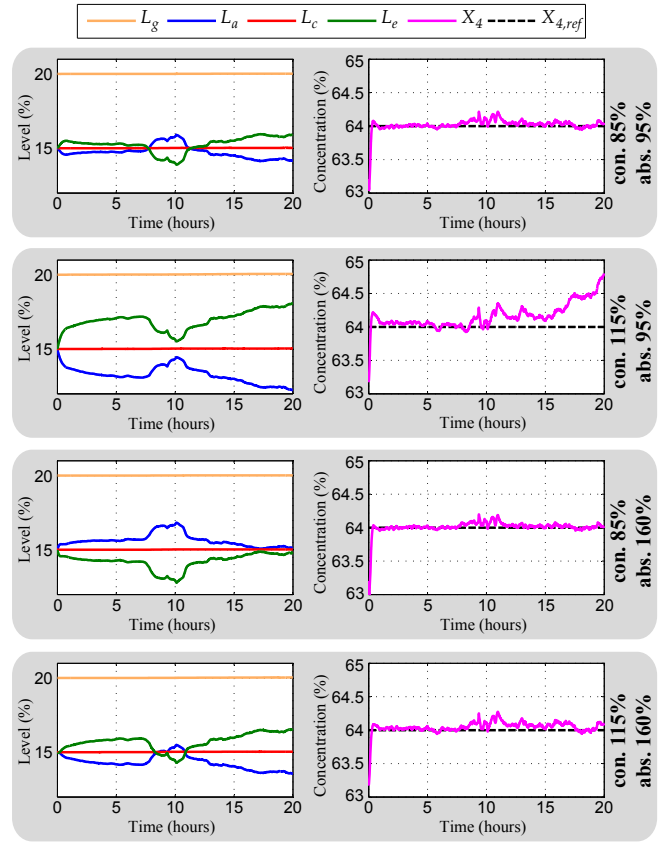

Fig. 8. Levels and concentration in simulations on the heat pump model using extreme external absorber and condenser water mass flow situations relative to their nominal scalings. From top to bottom: low condenser and low absorber flow, high condenser and low absorber flow, low condenser and high absorber flow, high condenser and high absorber flow.

VI. LINEARIZATION OF NONLINEAR MODEL FOR CONTROL DESIGN

The nonlinear heat pump model implemented in *Modelica* has the following states: four levels (4), temperature and concentration in absorber and generator (4), pressure and enthalpy for each volume element in the four main component HEXs (56), temperature of each volume element and each wall segment for the solution HEX (21, no pressure loss assumed), temperature of each wall segment and each volume element internally in the water HEX (14, no pressure loss assumed), pressure and enthalpy for each volume element externally in the water HEX (14). This gives 113 states.

A linear lower order model is often preferred for control design and *Dymola* has a built-in linearization functionality, which can linearize the nonlinear model in a given operating point. The output is a state space representation, where model order reduction can be performed on the high order model for the input/output set of interest, e.g., using the *Matlab* function `balred`. The linear model can be verified by perturbing the inputs of the nonlinear model with sinusoidal signals of different frequency and calculating the response in each output of interest. The test frequencies should be chosen around the desired control bandwidth as lower/higher frequencies are not as important for the control design.

terms of keeping the concentration at the reference and maintaining decent levels in the evaporator and the absorber. This is due to a too efficient condenser that overflows the evaporator with condensate, while the absorber does not absorb enough steam from the evaporator to maintain a healthy liquid level, which raises the concentration in the absorber and causes the concentration in the generator to raise as well. Note that generally in order to keep the evaporator and the absorber levels controlled at their nominal values (15%) it would be necessary to measure or estimate at least one of these levels, see [18]. However, the system is operable with suitable scaling of external mass flows.
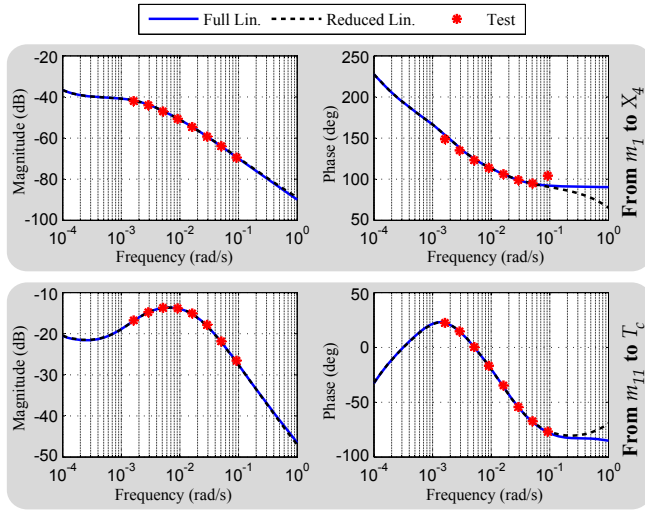
Fig. 9. Frequency response of a full order and a reduced order linear model of the SISO systems from solution mass flow m_1 to concentration X_4 (top graph) and from water mass flow m_{11} to condensation temperature T_c. The frequency response from tests is performed on the full nonlinear model.

The solution pump mass flow m_1 and the external generator water mass flow m_{11} are two internal inputs in the heat pump model. These inputs are used to control the generator outlet LiBr concentration X_4 and the condensation temperature T_c (or pressure) as described in Section IV. Fig. 9 shows the frequency response for the case with m_1 as input and X_4 as output and the case with m_{11} as input and T_c as output. Both full 113 order linear models, reduced order linear models (6. and 5. order, respectively), and test on the nonlinear model are shown for comparison.

The chosen orders gives a good fit for the presented frequency range, where only a small discrepancy in phase is observed for high frequencies (the *Matlab* function hsvd can also help indicate a suitable model order). The test also indicates that the linear model is a good approximation of nonlinear model, at least close to the chosen operating point (the amplitude of the sinusoidal perturbations are 5% of the nominal input at the operating point). However, note that any cross coupling effect from other inputs are lost, which means that either the chosen input should have a dominating effect on the chosen output or model reduction should be performed on a MIMO model with all inputs to the system.

VII. Conclusion

A nonlinear dynamic model of a single-effect absorption heat pump cycle has been derived for simulation and control design purposes and implemented in *Modelica*. The object oriented component modeling in *Modelica* makes it easy to extend the model and build more complex systems. A simple control setup for the heat pump is also provided, which is close to the control used in the plant at SFJV and can serve as a benchmark for more advanced control. Simulation using manually fitted model parameters have shown good agreement with 20 hours of closed-loop operational data in steady state and during a change in heat pump capacity

utilization. Simulation of different scenarios of external water flow control revealed potential problems when the condenser flow is high and the absorber flow is low. Furthermore, the potential for deriving reduced order linear models for control design is demonstrated through examples with two interesting input-output control pairs. Finally, the model has been used in a companion paper to analyze different input-output pairings in terms of control potential.

References

[1] Y. Man, H. Yang, and Z. Fang, "Study on hybrid ground-coupled heat pump systems," *Energy Build.*, vol. 40, no. 11, pp. 2028–2036, 2008.

[2] W. Yu, C. Zhu, and M. Gao, "An office building energy-saving design of ground source heat pump system," *Appl. Mech. and Mater.*, vol. 353-354, pp. 3093–3096, 2013.

[3] B. Wille-Haussmann, T. Erge, and C. Wittwer, "Decentralised optimisation of cogeneration in virtual power plants," *Sol. Energy*, vol. 84, no. 4, pp. 604–611, 2010.

[4] V. Verda and F. Colella, "Primary energy savings through thermal storage in district heating networks," *Energy*, vol. 36, no. 7, pp. 4278–4286, 2011.

[5] R. Lazzarin and M. Noro, "Local or district heating by natural gas: which is better from energetic, environmental and economic point of views?" *Appl. Therm. Eng.*, vol. 26, no. 2-3, pp. 244–250, 2006.

[6] G. Streckiene, M. Vytautas, N. Andersen, and J. Katz, "Feasibility of chp-plants with thermal stores in the german spot market," *Appl. Energy*, vol. 86, no. 11, pp. 2308–2316, 2009.

[7] B. Rezaie and M. Rosen, "District heating and cooling: review of technology and potential enhancements," *Appl. Energy*, vol. 93, pp. 2–10, 2012.

[8] K. E. Herold, R. Radermacher, and S. A. Klein, *Absorption Chillers and Heat Pumps*. CRC Press, 1996.

[9] P. Srikhirin, S. Aphornratana, and S. Chungpaibulpatana, "A review of absorption refrigeration technologies," *Renewable Sustainable Energy Rev.*, vol. 5, no. 4, pp. 343–372, 2001.

[10] S. Jeong, B. Kang, and S. Karng, "Dynamic Simulation of an Absorption Heat Pump for Recovering Low Grade Waste Heat," *Appl. Therm. Eng.*, vol. 18, no. 1-2, pp. 1–12, 1998.

[11] D. G. Fu, G. Poncia, and Z. Lu, "Implementation of an object-oriented dynamic modeling library for absorption refrigeration systems," *Appl. Therm. Eng.*, vol. 26, no. 2-3, pp. 217–225, 2006.

[12] J. Sun, lin Fu, S. Zhang, and W. Hou, "A mathematical model with experiments of single effect absorption heat pump using LiBr-H2O," *Appl. Therm. Eng.*, vol. 30, no. 17-18, pp. 2753–2762, 2010.

[13] Y. Shin, J. A. Seo, H. W. Cho, S. C. Nam, and J. H. Jeong, "Simulation of dynamics and control of a double-effect LiBr-H2O absorption chiller," *Appl. Therm. Eng.*, vol. 29, no. 13, pp. 2718–2725, 2009.

[14] A. Iranmanesh and M. Mehrabian, "Dynamic simulation of a single-effect LiBr-H2O absorption refrigeration cycle considering the effect of thermal masses," *Energy Build.*, vol. 60, pp. 47–59, 2013.

[15] Modelica Association. (2014, Jun.) Modelica libraries. [Online]. Available: https://modelica.org/libraries

[16] K. J. Åström and R. D. Bell, "Drum-boiler dynamics," *Automatica*, vol. 36, no. 3, pp. 363–378, 2000.

[17] J. Pátek and J. Klomfar, "A computationally effective formulation of the thermodynamic properties of LiBrH2O solutions from 273 to 500K over full composition range," *Int. J. Refrig.*, vol. 29, no. 4, pp. 566–578, 2006.

[18] K. Vinther, R. J. Nielsen, K. M. Nielsen, P. Andersen, T. S. Pedersen, and J. D. Bendtsen, "Analysis of Decentralized Control for Absorption Cycle Heat Pumps," in *ECC*, Linz, Austria, July 2015, in press.

[19] Hope Deepblue Air Conditioning Manufacture Corp., Ltd. (2014, Sep.) Hot water-type libr absorption chiller. [Online]. Available: http://www.slhvac.com/productsinfo.aspx?NId=8&NodeID=15

[20] R. Franke, F. Casella, M. Otter, M. Sielemann, H. Elmqvist, S. E. Mattson, and H. Olsson, "Stream Connectors - An Extension of Modelica for Device-Oriented Modeling of Convective Transport Phenomena," in *Modelica Conf.*, Como, Italy, September 2009, pp. 108–121.